Heavy-Higgs-boson production and vector-boson scattering processes in e^+e^- collisions at high energy

A. Tofighi-Niaki and J. F. Gunion
Department of Physics, University of California, Davis, California 95616
(Received 11 April 1988)

We study the reactions $e^-e^+ \to \nu\bar{\nu}ZZ$ and $e^-e^+ \to e^-e^+ZZ$ using exact matrix elements. In particular, we examine the cross section for the production of a standard-model Higgs boson at several machine energies. In addition, we study the behavior of the vector-boson scattering processes when the Higgs-boson mass is infinite, focusing on the percentage of longitudinally polarized Z's as a signature.

I. INTRODUCTION

In Ref. 1 (hereafter referred to as I) we considered the processes

$$e^-e^+ \to \nu\bar{\nu}W^-W^+ \tag{1}$$

and

$$e^-e^+ \to e^-e^+W^-W^+ , \tag{2}$$

using exact matrix elements. The primary motivation there was to investigate the observability of the Higgs boson of the minimal standard model, and to assess the extent to which the W^-W^+ scattering continuum might be measurable away from the Higgs-resonance region or in the instance that the Higgs-boson mass m_H is very large. Related work using some form of approximation has also appeared.[2-8] (Typical approximations are to compute using the effective W technique or to keep only the Higgs-resonance contribution in an "on-pole" approximation. Prior to I exact matrix elements had only been employed in hadronic collider studies.[9]) At the energies investigated, Higgs-boson observation appears to be fairly straightforward once techniques to eliminate backgrounds, especially those from the two-photon diagrams contributing to reaction (2) and beamstrahlung degradation of continuum $e^-e^+ \to W^-W^+$ production, are implemented. This has been further studied using realistic Monte Carlo simulations in Ref. 10. In contrast, separation of the W^-W^+ scattering continuum from the various background processes also producing W^-W^+ pairs appeared to be difficult.

In this paper we investigate the closely allied processes

$$e^-e^+ \to \nu\bar{\nu}ZZ \tag{3}$$

and

$$e^-e^+ \to e^-e^+ZZ . \tag{4}$$

If sufficient mass resolution is available to distinguish between W's and Z's in their hadronic decay modes (in the purely leptonic modes it is obviously possible to separate these two final states, but the event rates are low), then the ZZ final state has very definite advantages. In particular, there are no two-photon diagrams contributing to reaction (4). The only diagrams in which a nearly on-shell photon emission is possible are those in which the e^+ (say) emits an on-shell photon which then participates in the subprocess $\gamma + e^- \to e^- + ZZ$. In addition, the Z's themselves are weakly coupled to electrons and positrons, implying that the above type of subprocess is itself not large. Indeed, all diagrams contributing to (4) contain Z couplings to electrons or positrons. As a result, we find that the cross section coming from (4) is always small compared to that from reaction (3). The most important background will then derive from $e^+e^- \to ZZ$ occurring at less than full machine center-of-mass energy due to beamstrahlung emissions of the colliding e^+ and e^-. However, at a given invariant mass for the ZZ pair, the cross section for $e^-e^+ \to ZZ$ is generally smaller by more than a factor of 10 than that for $e^-e^+ \to W^-W^+$ for the equivalent WW pair mass. In contrast, we shall see that the cross section for the ZZ final state from reaction (3) is not much smaller than that for the W^-W^+ final state from reaction (1). This is true whether or not the Higgs resonance is present. Thus, the beamstrahlung-induced background of ZZ pairs will be much less severe than the corresponding background of WW pairs, relative to the vector-boson scattering signals of interest. In particular, the techniques used in Ref. 10 to isolate the signals of interest in the W^-W^+ final state in the presence of such a background should be even more effective for the ZZ final state.

In this paper our emphasis will be twofold. First, we shall give ZZ cross sections in the presence of the Higgs resonance; second, we shall investigate the ZZ continuum away from the Higgs resonance. In both cases we shall compare them to the corresponding results for the W^-W^+ final state. Second, we shall compute the fraction of Z's in the final state of reaction (3) that are longitudinally polarized at high M_{ZZ} invariant mass. From both a theoretical and an experimental viewpoint, this will prove to be especially interesting when the Higgs-boson mass is much larger than M_{ZZ}, and continuum $W^-W^+ \to ZZ$ scattering processes dominate. In particular, we shall determine what machine energies are required in order for the longitudinal-polarization signature of the perturbative calculation to become prominent at

large M_{ZZ}, and we will provide a precise standard of comparison against which to judge possible nonperturbative modifications. In addition, our analysis makes it possible to assess the extent to which projecting against transversely polarized Z's might be able to isolate the $W^-W^+ \to ZZ$ scattering continuum from other continuum ZZ pair production processes, given that the latter produce mainly transversely polarized Z's. Of special interest will be comparisons between the ZZ and W^-W^+ final state. We shall demonstrate that rapidity cuts on the outgoing vector bosons are very necessary in the case of the W^-W^+ final state in order to reveal the longitudinal nature of the underlying $W^-W^+ \to W^-W^+$ scattering process at high M_{WW}, whereas for the ZZ final-state rapidity cuts are not essential, merely helpful. These are important issues since accessing and understanding the high-M_{ZZ},M_{WW} region of continuum $W^-W^+ \to ZZ$, W^-W^+ scattering at a TeV e^+e^- collider will be vital, especially if the Higgs boson is very heavy.

II. OVERVIEW OF TECHNICAL DETAILS

Our computation employs exact matrix elements deriving from all diagrams contributing to reactions (3) and (4), computed using the spinor techniques of Ref. 11. [The results for the matrix elements of processes (1)–(4) will be published elsewhere.[12] The amplitudes for all the contributing diagrams can be expressed in terms of just a few fundamental spinor functions.] In this technique, the final Z's are automatically decayed to massless fermions, and an integration over six-body final-state phase space is performed. This allows a realistic simulation of experimental observables, such as the decay angle θ^* of a fermion pair computed in the Z rest frame and defined with respect to the direction of the boost required to give the Z its actual laboratory momentum.[13] Since the work of I we have also vastly improved the speed of the Monte Carlo program, by generating events with emphasis on the small angle regions for the $\nu\bar{\nu}$ spectators in reaction (3). As a result we can now explore energies above $\sqrt{s}=1$ TeV using modest amounts of computer time.

III. CROSS SECTIONS FOR HIGGS-BOSON PRODUCTION AND THE ZZ CONTINUUM

It will be convenient to refer to a standard integrated luminosity for the e^-e^+ collider defined by

$$L=\frac{10^4 l}{\sigma_{\rm pt}} , \tag{5}$$

where $\sigma_{\rm pt}$ is the cross section for $e^-e^+ \to \gamma^* \to \mu^-\mu^+$. This is the same as

$$L=(1.15l\times 10^5\ {\rm pb}^{-1})[\sqrt{s}\ ({\rm TeV})]^2 .$$

For a theorist's year of 10^7 sec, it is equivalent to an instantaneous luminosity of

$$\mathcal{L}=(1.15l\times 10^{34}\ {\rm cm}^{-2}{\rm sec}^{-1})[\sqrt{s}\ ({\rm TeV})]^2 . \tag{6}$$

In parallel with I we examine in detail three cases in which the Higgs boson should prove observable:

(i) $m_H=300$ GeV ($\Gamma_H=9$ GeV) at $\sqrt{s}=500$ GeV ;

(ii) $m_H=500$ GeV ($\Gamma_H=52$ GeV) at $\sqrt{s}=1$ TeV ;

(iii) $m_H=1$ TeV ($\Gamma_H=468$ GeV) at $\sqrt{s}=2$ TeV .

Our results for the M_{ZZ} spectra arising from reaction (3) are presented in Fig. 1. The spectra are, of course, quite similar to those obtained in I for reaction (1), using the same rapidity cuts. In particular, at the peak of the Higgs resonance, a comparison with the results for (1) yields $d\sigma/dM_{ZZ} \simeq \frac{1}{2} d\sigma/dM_{WW}$, as anticipated on the basis of standard Higgs-boson couplings to VV pairs and the identical particle factor required for the ZZ final state. We may continue this comparison by computing the number of events in the Higgs-boson mass peak (defined as the difference between the spectrum for a given Higgs-boson mass and that at the same energy for $m_H=\infty$) obtained by integrating over M_{ZZ}. We find

$$\text{No. of events in Higgs-boson peak}=\begin{cases} 85l: & m_H=0.3\ \text{TeV},\ \sqrt{s}=0.5\ \text{TeV} , \\ 793l: & m_H=0.5\ \text{TeV},\ \sqrt{s}=1\ \text{TeV} , \\ 3596l: & m_H=1\ \text{TeV},\ \sqrt{s}=2\ \text{TeV} , \end{cases} \tag{7}$$

to be compared to 196l, 1551l, and 6062l for reaction (1) (Ref. 14). The Higgs-boson cross sections corresponding to the above numbers are $2.99(6.83)\times 10^{-3}$ pb in case (i); $6.90(13.49)\times 10^{-3}$ pb in case (ii); and $7.82(13.18)\times 10^{-3}$ pb in case (iii); where the numbers in parentheses correspond to the WW channel and those outside to the ZZ channel.

Turning to the $m_H=\infty$ continuum for reaction (3), we parallel I by computing the number of events obtained by integrating over M_{ZZ} from: 0.2 to 0.4 TeV in case (i); 0.3 to 0.7 TeV in case (ii); and 0.5 to 1.5 TeV in case (iii). We obtain

$$\text{No. of } ZZ \text{ continuum events}=\begin{cases} 12l: & 0.2<M_{ZZ}({\rm TeV})<0.4,\ \sqrt{s}=0.5\ \text{TeV} , \\ 383l: & 0.3<M_{ZZ}({\rm TeV})<0.7,\ \sqrt{s}=1\ \text{TeV} , \\ 5169l: & 0.5<M_{ZZ}({\rm TeV})<1.5,\ \sqrt{s}=2\ \text{TeV} , \end{cases} \tag{8}$$

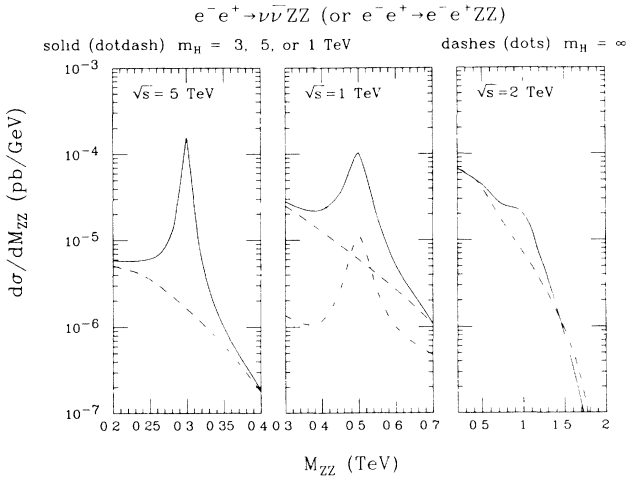

FIG. 1. The spectrum $d\sigma/dM_{ZZ}$ from reaction (3) as a function of M_{ZZ}, for the three cases specified in the text. We have required that all outgoing Z decay products have center-of-mass (i.e., laboratory) rapidity $y<4$. The solid curves correspond to $m_H=0.3$, 0.5, or 1 TeV, depending on case, while the dashed curves correspond to $m_H=\infty$. Also given in the $\sqrt{s}=1$ TeV graph are results for reaction (4), using dotted-dashed and dotted curves for the $m_H=0.5$ TeV and $m_H=\infty$ cases, respectively.

to be compared to $32l$, $761l$, and $7726l$ events in the WW continuum from reaction (1), as given in I. As mentioned in the Introduction, the integrated ZZ continuum cross section is a substantial fraction of that for WW pairs—as much as $\frac{2}{3}$ at the highest energy considered.

Let us now make a few brief remarks about reaction (4). We consider the $m_H,\sqrt{s}$ case (ii) for purposes of illustration. In the $\sqrt{s}=1$ TeV window of Fig. 1 the $d\sigma/dM_{ZZ}$ spectrum from reaction (4) is presented for comparison with the corresponding one from reaction (3). The small size of the former is immediately apparent. It should be recalled that this same comparison for the W^-W^+ final state resulted in a much larger cross section for reaction (2) than for (1), due to the contributions to (2) from $\gamma\gamma\to W^-W^+$ subprocesses. This caused a severe continuum background to the $W^-W^+\to W^-W^+$ subprocesses of interest contained in reaction (1). Here there is clearly no such difficulty.

Next we consider the effects on the above results of cuts that might be useful in reducing backgrounds. In particular, as described in I and Ref. 10, there are two types of cuts that are particularly effective in eliminating backgrounds from $e^-e^+\to VV$ due to beamstrahlung degradation of the e^-e^+ effective energy. These same cuts also serve to eliminate a variety of other sources of VV continuum pair backgrounds. The cuts consist of requiring $y_V<1.5$ for each of the outgoing vector bosons, and requiring $p_T^{VV}>p_T^{\min}$ for the net transverse momentum of the VV pair. The value of $p_T^{\min}$ is optimized for a given case. In addition, since the spectators to VV pair production in reactions (3) and (1) are invisible, backgrounds that have spectators [such as reactions (4) and (2)] contribute only to the extent that the spectators are not observable. The degree to which one is unable to observe these spectators depends upon detector and machine specifications. Sample criteria are outlined in I and Ref. 10. As an example of the effect of the p_T^{VV} and y cuts on the reaction (3), let us consider case (ii), with $\sqrt{s}=1$ TeV, and take $M_{ZZ}=0.5$. After imposing the above cuts with $p_T^{\min}=90$ GeV, we obtain

$$\frac{d\sigma}{dM_{ZZ}}=3.95\times10^{-5}\ \frac{\text{pb}}{\text{GeV}}\quad\text{for } m_H=0.5\text{ TeV},$$
$$\frac{d\sigma}{dM_{ZZ}}=2.83\times10^{-6}\ \frac{\text{pb}}{\text{GeV}}\quad\text{for } m_H=\infty\ . \tag{9}$$

These are slightly less than one-half the corresponding values in the absence of cuts, as can be seen from Fig. 1. [The corresponding $d\sigma/dM_{ZZ}$ values for reaction (4) after imposing the above cuts and requiring that the final-state e^-e^+ spectators be unobservable (see the criteria in I) are more than a factor of 200 smaller.] Thus, such cuts are relatively efficient in retaining the processes of interest, while, as described in I and Ref. 10, they are highly effective in eliminating backgrounds. A detailed Monte Carlo study is required to determine if the background in the ZZ case is reduced to a sufficiently low level that the $WW\to ZZ$ scattering continuum can be studied. As mentioned earlier, the situation is marginal in the WW channel. However, we have seen above that the ZZ channel could prove less difficult. Certainly, it will be extremely important to be able to measure the level of the $WW\to ZZ$ scattering continuum in the $M_{ZZ}\sim1$ TeV region if the Higgs resonance lies at still higher masses.

IV. THE FRACTION OF LONGITUDINALLY POLARIZED Z's

As emphasized in many places, including Ref. 15, I, and Ref. 7, an important signature for Higgs-boson production, or for the onset of strong interactions in $VV\to VV$ scattering processes should the Higgs-boson mass be very large, is a dramatic increase in the fraction of longitudinally polarized vector bosons produced. This can be detected in at least two ways.

(1) By a change to a $\sin^2\theta^*$ distribution (for the V decay products in the V rest frame) characteristic of a longitudinally polarized V, from the $(1\pm\cos\theta^*)^2$ distribution typical of a transversely polarized V. (The angle θ^* was defined in Sec. II.)

(2) By a change in the $r_T^{\min}$-$r_T^{\max}$ distribution for the V decay products, where

$$r_T^{\max}=\frac{p_T^{\max}}{M_{VV}},\quad r_T^{\min}=\frac{p_T^{\min}}{M_{VV}}\ , \tag{10}$$

are defined using the larger and smaller transverse momenta of the V decay products in the VV center of mass, respectively.

The latter technique was described in some detail in I. Here we shall analyze the fraction of longitudinally polarized Z's in reaction (3) by employing a projection operator technique[16] in $\cos\theta^*$. In this technique we com-

pute for a given M_{ZZ} the fraction f_L of Z's that have longitudinal polarization as

$$f_L \equiv \frac{\int_{-1}^{1} d\cos\theta^* \frac{d^2\sigma}{dM_{ZZ}d\cos\theta^*}(2-5\cos^2\theta^*)}{\int_{-1}^{1} d\cos\theta^* \frac{d^2\sigma}{dM_{ZZ}d\cos\theta^*}} . \quad (11)$$

If the cross section takes the form

$$\frac{d\sigma}{dM_{ZZ}d\cos\theta^*} = A\sin^2\theta^* + B(1+\cos^2\theta^*) , \quad (12)$$

corresponding to a superposition of longitudinally and transversely polarized Z's, f_L isolates exactly the fraction of the $\cos\theta^*$-integrated cross section deriving from the longitudinal component. We have performed this projection on only one of the outgoing Z's.

Before quoting results for f_L it is useful to plot a few raw distributions in $\cos\theta^*$ for the W^-W^+ and ZZ final states of reactions (1) and (3). We have chosen to give these plots for M_{WW} or M_{ZZ} at 1.2 TeV and $\sqrt{s}=2$ TeV. For each final state we show four separate distributions: (a) $m_H=0.8$ TeV, no y cut; (b) $m_H=\infty$, no y cut; (c) $m_H=0.8$ TeV, $y<1.5$ required for both W's or Z's; and (d) $m_H=\infty$, $y<1.5$ required for both W's or Z's. In the case of the Z, we give results for purely left-handed coupling of the decay fermion (as would be appropriate for $Z\to\nu\bar{\nu}$) in order to allow cleanest comparison to the W case. The distributions appear in Fig. 2 for the WW case and Fig. 3 for the ZZ case. It is apparent from these graphs that the longitudinally polarized W components of the $\cos\theta^*$ distributions are totally obscured in the case of the WW final state when no rapidity cut is applied, whereas in the case of the ZZ final state a large longitudinal-polarization component is already evident before imposing the rapidity cut. We believe that this is due to the larger number of diagrams (in particular photon-exchange diagrams) that contribute to the WW final state, but do not produce longitudinally polarized W's, in comparison to the ZZ case. These diagrams are greatly suppressed by the rapidity cuts on the outgoing vector bosons. We note that the figures in Ref. 7 which

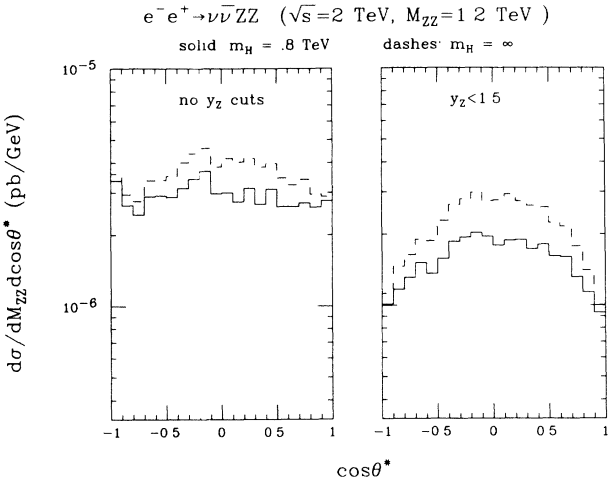

FIG. 3. Distributions in $\cos\theta^*$ for one of the outgoing Z's in reaction (3). In the first pair of graphs, no cut on the outgoing Z rapidities has been imposed. In the second $y_Z<1.5$ is required for both Z's. In both cases we have taken $\sqrt{s}=2$ TeV, $M_{ZZ}=1.2$ TeV, and given results for $m_H=0.8$ TeV and $m_H=\infty$. The distributions are those for a purely left-handed coupling of the Z decay products (i.e., those that would be appropriate for $Z\to\nu\bar{\nu}$).

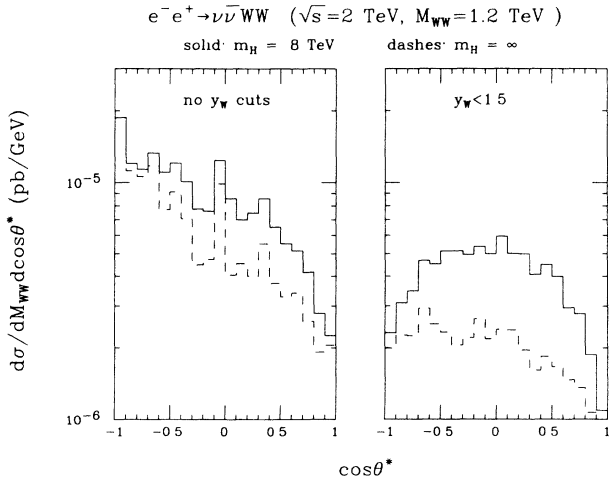

FIG. 2. Distributions in $\cos\theta^*$ for one of the outgoing W's in reaction (1). In the first pair of graphs, no cut on the outgoing W rapidities has been imposed. In the second $y_W<1.5$ is required for both W's. In both cases we have taken $\sqrt{s}=2$ TeV, $M_{WW}=1.2$ TeV, and given results for $m_H=0.8$ TeV and $m_H=\infty$.

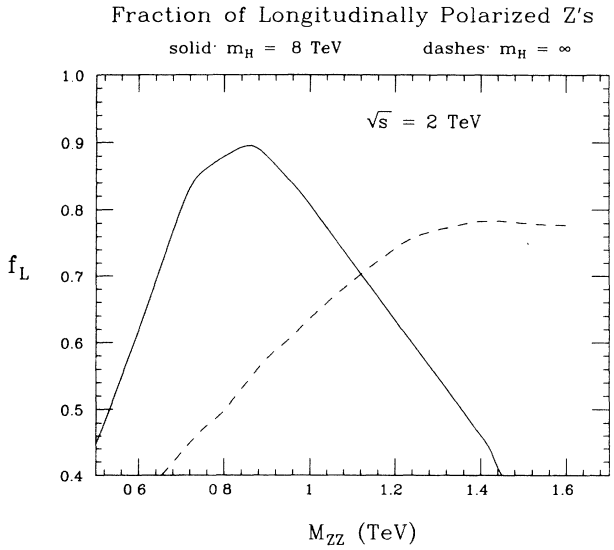

FIG. 4. The fraction f_L of longitudinally polarized Z bosons in the final state of reaction (3) as a function of M_{ZZ}. We have taken $\sqrt{s}=2$ TeV, and plot results for $m_H=0.8$ TeV (solid curve) and $m_H=\infty$ (dashed curve). We have imposed a rapidity cut of $y<1.5$ on both outgoing Z's.

indicate small longitudinal-polarization cross sections in WW scattering at $\sqrt{s}=2$ TeV have not included rapidity cuts, and are in rough agreement with what we find in the same case.

Let us now turn to the overall behavior of f_L. Here we shall present results only for the ZZ final state, imposing rapidity cuts of $y<1.5$ on both outgoing Z's. Results for the WW final state are similar, but not identical. Qualitatively, we know that at small values of M_{ZZ}, independent of the Higgs-boson mass so long as M_{ZZ} is not near m_H, the Z's in reaction (3) will be produced mainly with transverse polarization. However, as we increase M_{ZZ} the fraction f_L of longitudinally polarized Z's can either decrease or increase depending upon the location of the Higgs resonance. If the Higgs boson is kinematically accessible, f_L will peak at $M_{ZZ}\sim m_H$ and decrease for higher M_{ZZ}. If the Higgs boson is very heavy, then f_L will rise continuously as M_{ZZ} increases, possibly plateauing for sufficiently large M_{ZZ} values. These features are illustrated in Fig. 4, where we plot f_L as a function of M_{ZZ} at $\sqrt{s}=2$ TeV for $m_H=0.8$ TeV and $m_H=\infty$. We observe that for $m_H=0.8$ TeV the longitudinal fraction peaks at $M_{ZZ}=m_H$, and dies away for higher M_{ZZ} values. In contrast, if $m_H=\infty$ the longitudinal fraction rises continuously through the region where the cross section is sufficient to give a nontrivial number of events, plateauing at about 80%. Thus, in principle f_L can provide a powerful signal for separating and studying the $W^-W^+\to ZZ$ scattering subprocesses in the high M_{ZZ} domain. Of course, the event rate is not large at these high invariant masses. For instance, from Fig. 1 we see that at $M_{ZZ}=1.2$ TeV ($\sqrt{s}=2$ TeV) $d\sigma/dM_{ZZ}$ is of order 3×10^{-6} pb/GeV corresponding to only about $15l$ events per 10-GeV bin per year for the luminosity of Eqs. (5) and (6). Imposition of the $y<1.5$ cut reduces this number to about $10l$. Whether or not beamstrahlung-induced backgrounds from continuum $e^-e^+\to ZZ$ production and $e^-e^+\to W^-W^+$ (due to poor mass resolution in the latter case) can be brought below this level is a question that requires Monte Carlo study. The energy $\sqrt{s}=2$ TeV is roughly the minimum energy at which observation of the rising longitudinal fraction at high M_{ZZ} in the large m_H case is at all feasible. Indeed, at $\sqrt{s}=1$ TeV, Fig. 1 shows that we run out of events by $M_{ZZ}\sim0.7$ TeV, a point at which f_L only just begins its dramatic increase.

V. CONCLUSIONS

We have shown that the exact matrix-element calculations for Higgs-boson production in the process (3) agree with expectations based on the earlier effective W calculations. In addition, we have computed the ZZ pair continuum from reaction (3), which includes the vector-boson scattering subprocesses of the type $W^-W^+\to ZZ$ that are of particular interest if the Higgs-boson mass turns out to be very large. We obtain the important result that this ZZ pair continuum is only a factor of two-thirds smaller than the WW pair continuum resulting from reaction (1) at the lowest machine energy ($\sqrt{s}=2$ TeV) for which it might conceivably be experimentally accessible. Since the level of the beamstrahlung-induced ZZ pair production background is nearly a factor of 10 smaller than the corresponding WW pair background, measurement of vector-boson scattering processes using ZZ final states is probably significantly easier than for WW final states. Our calculations also demonstrate and confirm the importance of isolating longitudinally polarized Z's at high M_{ZZ} as a signal for the $W^-W^+\to ZZ$ scattering subprocess. Should the Higgs-boson mass be very large, this will be the best probe of this important aspect of standard-model physics at an e^-e^+ collider.

ACKNOWLEDGMENTS

We would like to thank G. Kane for helpful discussions. In addition, we gratefully acknowledge the assistance of J. Smith in designing an efficient Monte Carlo event generator for our computations. This work was supported in part by the Department of Energy.

[1]J. F. Gunion and A. Tofighi-Niaki, Phys. Rev. D **36**, 2671 (1987).

[2]S. Dawson and J. Rosner, Phys. Lett. **148B**, 497 (1984).

[3]K. Hikasa, Phys. Lett. **164B**, 385 (1985).

[4]G. Altarelli, B. Mele, and F. Pitolli, Nucl. Phys. **B287**, 205 (1987).

[5]M. C. Bento and C. H. Llewellyn Smith, Nucl. Phys. **B289**, 36 (1987).

[6]I. Nikolaus, Z. Phys. C **34**, 361 (1987).

[7]G. L. Kane and J. J. G. Scanio, Nucl. Phys. **B291**, 221 (1987).

[8]G. Altarelli *et al.*, in *Proceedings of the Workshop on Physics at Future Accelerators,* La Thuile, Italy, 1987, edited by J. H. Mulvey (CERN Report No. 87-07, Geneva, Switzerland, 1987), Vol. 1.

[9]The first exact matrix-element treatments for hadronic collisions appeared in J. F. Gunion, J. Kalinowski, and A. Tofighi-Niaki, Phys. Rev. Lett. **57**, 2351 (1986); D. A. Dicus, S. L. Wilson, and R. Vega, Phys. Lett. B **192**, 231 (1987). For a review of all exact matrix element treatments, see J. F. Gunion, H. E. Haber, G. L. Kane, and S. Dawson, Phys. Rep. (to be published).

[10]SLAC Study Group on the Physics of Mid-Hundred GeV to TeV e^+e^- Colliders report (in preparation). The Monte Carlo work by D. Burke and P. Burchat for neutral Higgs bosons is the most relevant for our purposes here.

[11]J. F. Gunion and Z. Kunszt, Phys. Lett. B **161**, 333 (1985), and references therein to related techniques developed by other authors.

[12]A. Tofighi-Niaki and J. F. Gunion (in preparation).

[13]We remark that one could also have chosen to define θ^* with respect to the Z direction in the ZZ center-of-mass frame; in practice, this makes very little difference in the distributions

obtained.

[14]We note that the event numbers quoted for the Higgs-boson peak in I were incorrectly computed. The numbers quoted here are the corrected results.

[15]M. Chanowitz and M. K. Gaillard, Nucl. Phys. **B261**, 379 (1985); M. Chanowitz, M. Golden, and H. Georgi, Phys. Rev. Lett. **57**, 2344 (1986).

[16]M. J. Duncan, G. Kane, and W. Repko, Nucl. Phys. **B272**, 517 (1986).